Diffusion properties of Gabonese tropical hardwoods and European softwoods measured with low-tech equipment and by an inverse method

Martian Asseko, Arthur Bontemps, Gael Godi, Rostand Moutou Pitti, Giacomo Goli, Samuel Ikogou, Éric Fournely, Joseph Gril

Diffusion properties of Gabonese tropical hardwoods and European softwoods measured with low-tech equipment and by an inverse method

Martian Asseko Ella[1]
Arthur Bontemps[1,6]
Gaël Godi[1]
Rostand Moutou Pitti[1,2]
Giacomo Goli[3]
Samuel Ikogou[4]
Éric Fournely[1]
Joseph Gril[1,5]

[1] Université Clermont Auvergne, CNRS, Clermont Auvergne INP, Institut Pascal, 63000 Clermont-Ferrand
France

[2] CENAREST, IRT
BP 14070, Libreville
Gabon

[3] University of Florence
DAGRI-Department of Agriculture, Food, Environment and Forestry
50145 Firenze
Italia

[4] USTM
École Polytechnique de Masuku
BP 901 Franceville
Gabon

[5] Université Clermont Auvergne, INRAE, PIAF
63000 Clermont Ferrand
France

[6] Univ Lyon, ECAM LaSalle, LabECAM
40 Montée Saint Barthélémy
69321 Lyon Cedex 05
France

Auteur correspondant / Corresponding author:
Arthur Bontemps – arthur.bontemps@ecam.fr

ORCID : https://orcid.org/0000-0002-5895-7222

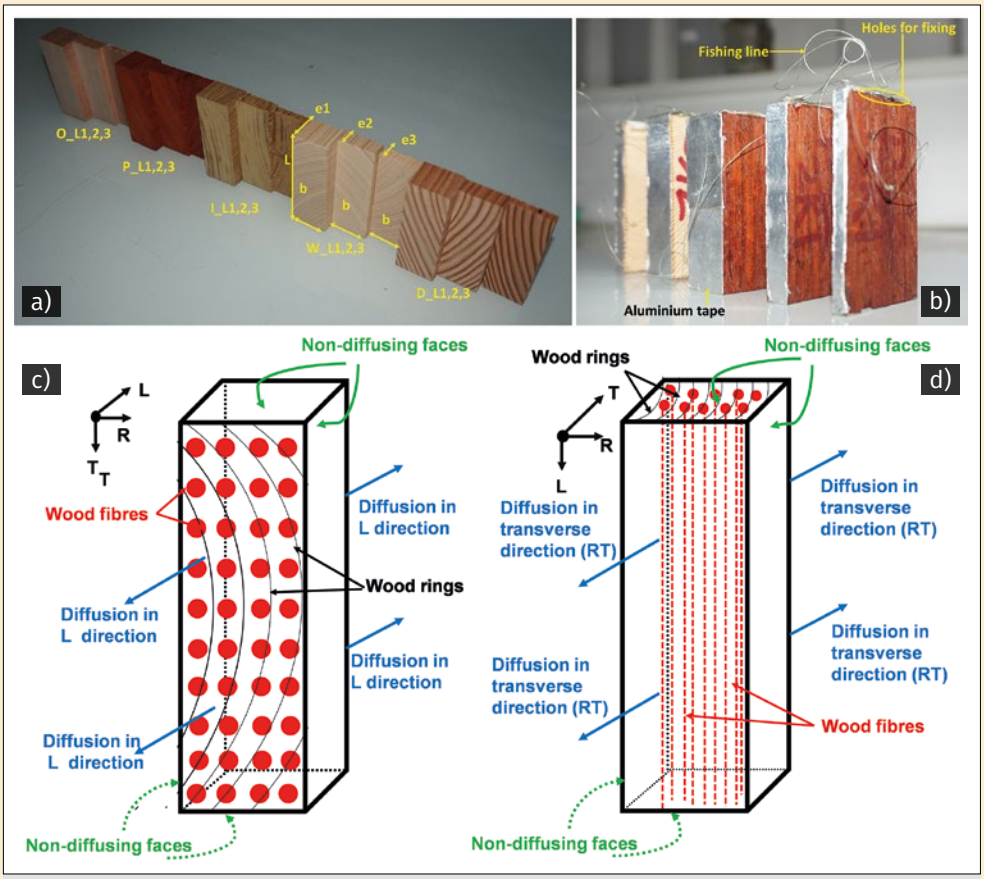

Figures 1.
Tested specimens: (a) different types and geometries of specimens; (b) specimens prepared with insulating tape (to allow a unidirectional diffusion) and fishing line (to be hanged during mass measurement); (c) geometry and direction of diffusion for specimens orientated in the L direction; (d) geometry and direction of diffusion for specimens orientated in the transverse direction RT.

Doi : 10.19182/bft2024.360.a37392 – Droit d'auteur © 2024, Bois et Forêts des Tropiques – © Cirad – Date de soumission : 19 janvier 2024 ; date d'acceptation : 21 mai 2024 ; date de publication : 1er juin 2024.

Citer l'article / To cite the article
Asseko Ella M., Bontemps A., Godi G., Moutou Pitti R., Goli G., Ikogou S., Fournely É., Gril J., 2024. Diffusion properties of Gabonese tropical hardwoods and European softwoods measured with low-tech equipment and by an inverse method. Bois et Forêts des Tropiques, 360 : 1-12. Doi : https://doi.org/10.19182/bft2024.360.a37392

Bois et Forêts des Tropiques – ISSN: L-0006-579X
Volume 360 – 2nd quarter – June 2024 – p. 1-12
RESEARCH / DIFFUSION PROPERTIES OF GABONESE TROPICAL HARDWOODS

M. Asseko Ella, A. Bontemps, G. Godi, R. Moutou Pitti, G. Goli, S. Ikogou, É. Fournely, J. Gril

RÉSUMÉ

Mesure de la diffusion dans le bois des feuillus tropicaux du Gabon et des résineux européens à l'aide de moyens à faible technicité et par méthode inverse

Cet article présente une approche expérimentale appliquée à l'étude des propriétés de sorption et de diffusion du bois. Cinq essences de bois - trois feuillus tropicaux africains, le padouk, l'okoumé et l'iroko, et deux résineux tempérés, le sapin blanc et le Douglas - ont été étudiées en mode adsorption. Des échantillons d'une épaisseur longitudinale (L) de 10 mm et transversale (RT) de 20 mm ont été imperméabilisés sur leurs côtés afin de forcer la diffusion dans ces directions. Après séchage, les échantillons ont été suspendus sous couvert par des fils de nylon dans une boîte fabriquée artisanalement dans laquelle des solutions salines assuraient une humidité relative (HR) constante, puis conditionnés par étapes successives à 43, 55, 75, 84 et 97 % HR, la température étant maintenue entre 20 et 24 °C. Au cours des étapes d'équilibrage, les échantillons ont été périodiquement pesés sans modifier les conditions environnementales imposées, en passant le fil de nylon à travers un petit trou dans le couvercle de la boîte pour suspendre l'échantillon à un peson. Les propriétés de l'isotherme de sorption et les paramètres de diffusion ont été obtenus par une méthode inverse basée sur l'optimisation d'un modèle 1D aux différences finies. Les paramètres obtenus montrent une corrélation décroissante entre le coefficient de diffusion et la densité, comme l'ont observé plusieurs auteurs dans la littérature. Ils illustrent également l'impact des extractibles sur les paramètres de l'isotherme de sorption. Ces résultats démontrent que les essences tropicales à forte densité ou à forte teneur d'extractibles se comportent très différemment des résineux européens, ce qui empêche l'utilisation pour ces essences des normes d'équilibre de l'Eurocode 5.

Mots-clés : Coefficient de diffusion, taux d'humidité d'équilibre, méthode aux différences finies, méthode inverse, essences tropicales, Gabon.

ABSTRACT

Diffusion properties of Gabonese tropical hardwoods and European softwoods measured with low-tech equipment and by an inverse method

This paper presents an experimental approach to studies of the sorption and diffusion properties of wood. Five timber species - three African tropical hardwoods, Padauk, Okoume and Iroko, and two temperate softwoods, Silver fir and Douglas fir - were studied in adsorption mode. Specimens with 10- and 20-mm longitudinal (L) and transverse (RT) thickness were waterproofed on their sides to force diffusion in those directions. After kiln drying, the specimens were hung with nylon wires under cover in a home-made box in which salt solutions provided constant relative humidity (RH) and conditioned at 43, 55, 75, 84, and 97% RH in successive steps. Temperature was maintained between 20 and 24 °C. During the equilibration steps, the samples were periodically weighed, without altering the environmental conditions imposed, by hanging the nylon wire to a spring gauge through a small hole in the box cover. The sorption isotherm properties and diffusion parameters were obtained using an inverse method based on optimisation of a 1D finite difference model. The parameters obtained show a decreasing correlation between diffusion coefficient and density, as observed by several authors in the literature. They also illustrate the impact of extractives on the sorption isotherm parameters. These results show that tropical species with high density or many extractives behave very differently to European softwoods, which impedes the application of Eurocode 5 equilibrium standards for these species.

Keywords: Diffusion coefficient, equilibrium moisture content, finite-difference method, inverse method, tropical timber species, Gabon.

RESUMEN

Propiedades de difusión de la madera dura tropical gabonesa y de la madera resinosa europea medidas con equipamiento de baja tecnología y método inverso

Este artículo presenta un enfoque experimental en los estudios de las propiedades de sorción y difusión de la madera. Se estudiaron en modo adsorción cinco especies de madera: tres maderas duras tropicales africanas, narra, ocume e iroco, y dos maderas resinosas de clima templado, abeto balsámico y abeto de Douglas. Se impermeabilizaron lateralmente muestras con un grosor de 10 mm longitudinal (L) y 20 mm transversal (RT) para forzar la difusión en estas direcciones. Después de un secado en horno las muestras se colgaron de hilos de nilón bajo cubierto en una caja construida a mano donde soluciones salinas proporcionaban una humedad relativa constante (RH), programada con RH del 43, 55, 75, 84 y 97 % en etapas sucesivas. La temperatura se mantuvo entre 20 y 24°C. Durante los pasos de equilibrado las muestras se pesaron periódicamente sin alterar las condiciones ambientales impuestas, colgando el hilo de nilón de un dinamómetro a través de una pequeña abertura en la cubierta de la caja. Las propiedades de sorción isoterma y los parámetros de difusión se obtuvieron utilizando un método inverso basado en la optimización de un modelo 1D de diferencia finita. Los parámetros obtenidos muestran una correlación decreciente entre el coeficiente de difusión y la densidad, lo que coincide con las observaciones de varios autores en la literatura. Esto también ilustra el impacto del material extractivo en los parámetros de sorción isoterma. Estos resultados muestran que las especies tropicales con elevada densidad o mucho material extractivo se comportan de forma diferente a las maderas resinosas europeas, lo que impide la aplicación de las normas de equilibrio del Eurocódigo 5 para estas especies.

Palabras clave: Coeficiente de difusión, contenido de humedad en equilibrio, método de diferencia finita, método inverso, especies madereras tropicales, Gabón.

Introduction

Wood is a hygroscopic material; its mechanical and physical properties depend highly on its water content (Merakeb et al. 2009; Liu et al. 2020; Engonga Edzang et al. 2020). The study of water transfer in porous material from a theoretical and experimental point of view has been widely addressed in the past (Stamm 1959; Comstock 1963; Rosen 1978; Siau and Avramidis 1996; Agoua et al. 2001) with formulations based on Fick's laws. In the wood, water is present in the form of free water, as liquid or vapour in the lumens, and as bound water in the cell walls (Kollman and Côté 1968; Varnier et al. 2020). Knowledge of water movement properties such as diffusion coefficients allows for better estimating the flux of water desorbed or adsorbed (Mouchot 2002). These properties are involved in several processes, such as wood drying and chemical treatment (Choong and Skaar 1972; Agoua and Perré 2010). A good characterisation of the diffusion process requires the development of reliable experimental techniques. To date, there are several techniques and experimental methods to monitor the evolution of moisture content (MC) in wood in transient and steady states, including the weighing method and electrical methods (Mouchot 2002). Some of these techniques sometimes require taking the wood out of the enclosure and weighing it on a scale to estimate its mass, which may disturb the MC history of the tested specimens.

Studies on the hydric behaviour of tropical woods are still quite rare in the literature. Manfoumbi Boussougou et al. (2014) addressed the use of Eurocode 5 in the verification of wood constructions and their dimensioning in tropical environments. Alkadri et al. (2020) measured the hygromechanical properties of Grenadilla wood (*Dalbergia melanoxylon*); Simo-Tagne et al. (2016) can also be mentioned. These different studies are still insufficient and do not provide useful information to improve the correct use of tropical woods and promote their use. This makes it difficult to integrate tropical woods into construction projects, as the application of current recommendations such as Eurocode 5 does not consider the hydric properties of tropical woods in given contexts (Benoit et al. 2019). This is justified by the lack of data on tropical woods in the literature.

The purpose of this paper is twofold: to propose an experimental approach for transient mass monitoring of wood specimens and to characterise the hydric properties of three tropical species in comparison to two temperate references. The experimental setup allows measurements to be made on many specimens without disturbing the water status of the system in which the specimens are placed.

Material and Methods

Material

The work was carried out on a total of 60 wood specimens, including 3 tropical hardwoods, Okoume (O, *Aucoumea klaineana*), Padauk (P, *Pterocarpus soyauxii*), and Iroko (I, *Milicia excelsa*), and 2 temperate softwoods, Silver fir (SF, *Abies alba*) and Douglas fir (DF, *Pseudotsuga menziesii*). These specimens are installed into a test box with relative humidity (RH) regulated using saline solutions, itself placed in a room regulated in temperature (T) at about 20 °C.

The tests were performed on wood specimens of different thicknesses: *e*1 = 20 mm and *e*2 = 10 mm, as shown in figure 1a. The thinnest specimens (*e3* = 5 mm) are not used for further analysis because their mass measurements were too noisy. The measurements were carried out using a 100 g load cell. It was observed that the measurement system was unable to measure the masses of low-mass samples (around 4.3 ± 1.2 g) with sufficient accuracy. For each species, the thickness of the specimens was orientated along the longitudinal (L) or transverse (RT) direction; this latter designation means that no difference was made between the radial and tangential directions. To force the diffusion in the L or RT direction, the other 4 faces were covered with 3 layers of aluminium tape (figure 1b). On one of the upper sides of the test specimens, a space was left to attach to it a fishing line. Table I shows the dimensions and density of specimens tested in both directions. Density was measured after the samples were assumed stabilised in a constant environment of 20 °C and 43% relative humidity. The geometry and diffusion direction for specimens orientated in the L and RT directions are provided in figures 1c and 1d.

Table I.
Dimensions and density of tested specimens.

Specimen type	Thickness e (mm)	Width B (mm)	Length L (mm)	Density				
				Silver fir	Douglas fir	Okoume	Padauk	Iroko
L1	20	24	65	0.48 ± 0.01	0.49 ± 0.06	0.44 ± 0.01	0.50 ± 0.01	0.50 ± 0.01
L2	10							
RT1	20							
RT2	10							

Bois et Forêts des Tropiques – ISSN: L-0006-579X
Volume 360 – 2nd quarter – June 2024 – p. 1-12

Nomenclature

Abbreviations (straight letters):

DF	Douglas fir
EMC	Equilibrium moisture content [%]
FSP	Fiber saturation point
I	Iroko
L	Longitudinal direction
MC	Moisture content
O	Okoume
P	Padauk
RH	Air relative humidity [%]
WRMS	Weighted root mean square
RT	Radial-tangential direction (transverse)
SF	Silver fir
T	Air temperature [°C]

Variables

$\underline{\underline{A}}$	Second-order tensor of the implicit-Euler matrix problem
a_{ad}, φ_{ad}	Empirical parameters for the adsorption isotherm
α, … , A	Mass measurement number, given as index
$\underline{b}$	Firs-order tensor of the implicit-Euler matrix problem
β, … , B	Humidity level number given either as index or as exponent
B	Height [mm]
D_x	Diffusion coefficient in x direction [m.s^{-2}]
$\overline{D}_j^n$	Geometric mean of the diffusion coefficient during time step n, at position j
e	Thickness [mm]
h	Half thickness [mm]
j = 1, … , J + 1	Node number of the meshed problem, given as index
k_{Dx}	Dimensionless coefficient of the exponential relation between D_x and w
L	Length [mm]
m	Mass of a specimen measured with the load cell [g]
m_0	Initial mass [g]
m_{01}	Oven-dry mass of a specimen [g]
m_{02}	Second oven-dry mass, the specimen being covered with aluminum tape [g]
m_p, m_q	Calibration masses [g]
n, … , N	Time number of the meshed problem, given as exponent
p, q, m	Measurements given by the force cell of the calibration masses and for a given specimen [mV.V^{-1}]
S_x	Surface exchange coefficient in the x direction [m.s^{-1}]
t	Time [s]
w_j^n, $\overline{w}$	Moisture content at time n and position, average moisture content [%]
w_e	Equilibrium moisture content [%]
w_{surf}	Moisture content on the surface of the test piece [%]
μ	Measurement given by the force cell for a given specimen (mV.V^{-1})
x	Spatial direction

Experimental setup

The experimental device (figure 2) consists of a Plexiglas box of dimensions 45 × 20 × 20 cm^3 for sample conditioning and a mobile arm equipped with a load cell for the manual measurement of the mass of the specimens at regular intervals. The range of the load cell is 100 g. The ambience of the box is controlled using the saturated salt solutions reported in table II. The boxes are equipped with a thermo-hygrometric sensor monitoring RH and T.

The experimental box was equipped with a fan to allow air circulation and ensure a uniform RH inside the box. It was turned off during mass measurements to avoid turbulence influencing the measurement. The box was also equipped with a metal grid to prevent the samples from falling into the salt solution tank. The samples were held in place by a fishing line exiting through 10 mm diameter holes in the top of the box, closed with conical silicone plugs locking the line in place. The cap of each sample was removed only for the duration of its mass measurement,

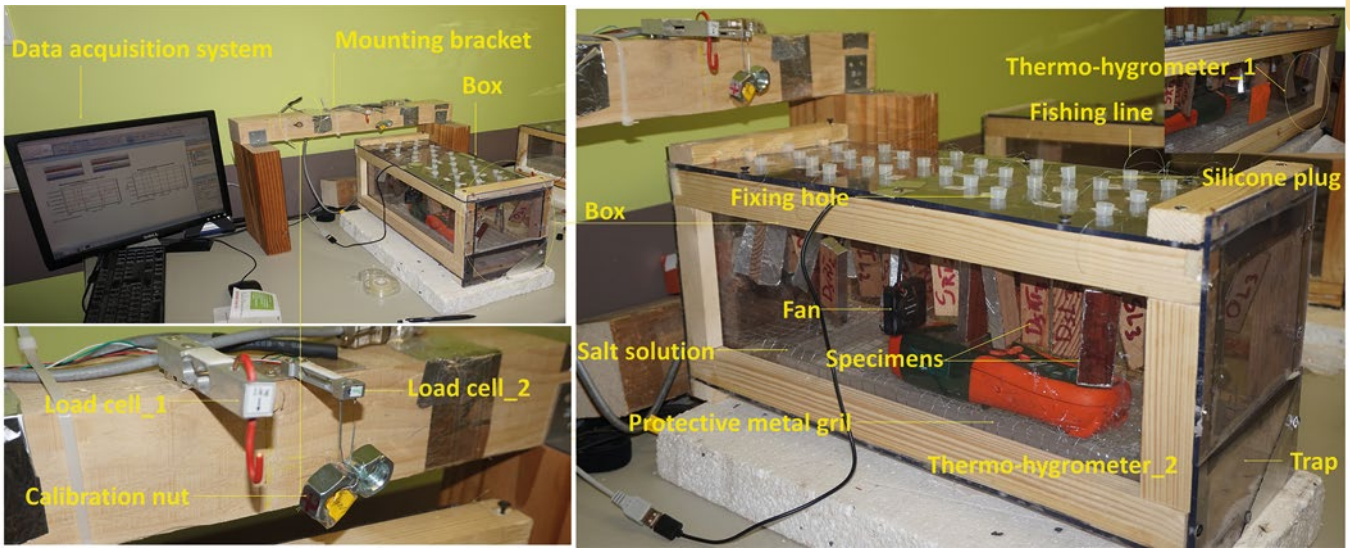

Figures 2.
Experimental setup for diffusion tests.

which greatly reduced air exchange between the inside of the box and the room. The box was conditioned using 6 salt solutions, according to the NF EN ISO 483 standard (2006), with expected RH levels of 43%, 57%, 75%, 84%, and 97%. The first step was to check the system reliability in conditioning the specimens at constant RH and T. Table II presents the values of RH and T observed in the box during the experimental phase. According to the standard, whether at T = 20 °C or T = 25 °C, we should find the same RH with the saline solutions used. This was confirmed by the results presented in table II: the RH values oscillated with a small standard deviation close to those expected by the standard, although small temperature variations occurred.

Sample preparation and mass measurement

After machining, the specimens were dried at 104 °C to estimate their oven-dry mass m_{01}. Once m_{01} was reached, the specimens were covered with adhesive aluminium tape and attached to a fishing line for later fixation. They were dried again at 104 °C to get a second oven-dry mass m_{02}, including tape and wire. After these two steps, the specimens were placed in the boxes for mass monitoring in a predefined order (O, P, SF, DF, I), starting with the specimens of the smallest thickness and moving toward the largest. Mass measurements were started as soon as possible from the beginning of each humidity level. The estimation of the mass m in grammes of a specimen was obtained by measuring the load cell output electrical signal m (in $mV.V^{-1}$) of a wooden specimen and those of two metal bolts used as calibration mass, p and q, given by the load cell (Equation 1):

$$m = m_p + \frac{m_q - m_p}{q - p}(\mu - p) \quad (1)$$

where m_p and m_q are the standard masses of the bolts previously determined on a precision balance (error less than 10^{-6} g). To avoid a possible drift, the calibration signals (p and q) are re-evaluated every 10 measurements using the reference masses (metal nuts). This procedure allowed an accuracy of 0,01% or 0,01 g, despite the use of a low-cost load cell. After obtaining the mass m, the evolution of the mean moisture content (MC, $\overline{w}$) of a specimen over time is given by (Equation 2):

$$\overline{w}(t) = \frac{m(t) - m_{02}}{m_{01}} \quad (2)$$

Diffusion model

During the previously described experiment, water vapour and bound water diffusion occur and these processes can be described, for a unidirectional flow along x direction, using second Fick's law (Equation 3):

$$\frac{\partial w}{\partial t} = \frac{\partial}{\partial x}\left(D_x \frac{\partial w}{\partial x}\right) \quad (3)$$

Table II.
Aqueous solutions used with expected relative humidity (RH) at temperature (T) of 20-25°C and measured climatic conditions.

Aqueous solution	RH (%) NF EN ISO 483	RH (%)	T (°C)
Potassium carbonate K_2CO_3	43	42.0 (± 0.4)	20.6 (± 0.5)
Sodium bromide NaBr	57	57.8 (± 1.1)	23.7 (± 0.5)
Sodium chloride NaCl	75	73.5 (± 1.3)	23.8 (± 0.4)
Potassium chloride KCl	84	83.4 (± 0.6)	23.9 (± 0.7)
Potassium sulfate K_2SO_4	97	94.8 (± 1.1)	23.3 (± 1.4)

where D_x is the diffusion coefficient in the direction of the water flow and w is the local MC, a function of position x and time t. The diffusion coefficient D_x depends on w. In the transverse direction, D_{RT} is exponentially increasing with w, while in the longitudinal direction D_L it is exponentially increasing at low w and then exponentially decreasing with w (Siau 1984). Neglecting the increasing part of D_L this can be expressed by (Equation 4):

$$D_{RT} = D_{RT0} . e^{k_{DRT} w} ; D_L = D_{L0} . e^{k_{DL} w} \quad (4)$$

where D_{RT0} and D_{L0} are the diffusion coefficient when $w = 0$, k_{DL} and k_{DRT} are the exponential factor relating D with w, k_{DL} being negative. Thybring et al. (2022) explain that phenomenon by the water mobility increasing when MC increases, possibly due to the decrease of the activation energy needed to break a hydrogen bond.

The boundary conditions use convection at one end and symmetrical geometry, leading to moisture content flux null at the other end. The convection process is described combining Newton's law for convection and first Fick's law (Equation 5):

$$D_x \frac{\partial w}{\partial x} = S(w_e - w_{surf}) \quad (5)$$

where S is the surface exchange coefficient, w_e and w_{surf} represent the equilibrium moisture content (EMC) and the sample surface's MC, respectively. w_e is the MC towards which wood MC tends in a given environment (RH, T). It follows a sorption hysteresis as it depends on the wood MC history and whether it is adsorbing or desorbing. The hysteresis is bounded by the so-called isotherm envelope, which was modelled by Merakeb et al. (2009) (Equation 6):

$$\ln\left(\frac{w_e}{w_s}\right) = \varphi_i \ln(RH) . e^{a_i . RH} \quad (6)$$

where w_s is the saturation MC, i.e., the Fiber Saturation Point (FSP), φ_i and a_i are empirical parameters that fit the isotherm envelopes. Considering only adsorption starting from $w = 0$, as it is the case in this study, $\varphi_i = \varphi_{ad}$ and $a_i = a_{ad}$. These 3 parameters depend on temperature and wood species. The symmetrical condition leads to $\partial w / \partial x = 0$.

Finite-difference approximation

A finite difference approximation is chosen to resolve the partial differential equation (3) as it is simple and efficient for 1D diffusion problems. A so-called θ-scheme is used with $\theta = 1/2$, corresponding to a Crank-Nicolson method that is unconditionally stable. Every sample is discretised in (J + 1) nodes (specified by index j) with a constant distance $\Delta x = x_j - x_{j-1} = 0.1$ mm. Time is specified using exponent n (N is the last instant), where the time step is refined when a humidity level is applied and then progressively unrefined until the next step, but never exceeding $\Delta t = 3600$ seconds. Mathematically, it can be written $\Delta t = \min(2^k, 3600)$ where $k = 1,2,3, \ldots, K$; and k is reset when a new humidity level starts. Equation (3) can hence be approximated by (Equation 7):

$$\frac{w_j^n - w_j^{n-1}}{\Delta t} = \frac{\theta}{\Delta x^2}\left[\overline{D}_{j+\frac{1}{2}}^{n-1}(w_{j+1}^n - w_j^n) - \overline{D}_{j-\frac{1}{2}}^{n-1}(w_j^n - w_{j-1}^n)\right] + \frac{(1-\theta)}{\Delta x^2}\left[\overline{D}_{j+\frac{1}{2}}^{n-1}(w_{j+1}^{n-1} - w_j^{n-1}) - \overline{D}_{j-\frac{1}{2}}^{n-1}(w_j^{n-1} - w_{j-1}^{n-1})\right] \quad (7)$$

where $\overline{D}_{j\mp\frac{1}{2}}^{n-1}$ is the geometric mean of the diffusion coefficient at time n - 1 and between x_j and $x_{j\pm1}$ (Equation 8):

$$\overline{D}_{j+1/2}^{n-1} = \sqrt{D_j^{n-1} . D_{j+1}^{n-1}}$$
$$\overline{D}_{j-1/2}^{n-1} = \sqrt{D_j^{n-1} . D_{j-1}^{n-1}} \quad (8)$$

where $D_j^{n-1} = D_0 . e^{k w_j^{n-1}}$. Note that the diffusion coefficient calculation remains explicit, whence $\Delta t \leq 3600$ to keep convergence. Using equation (5), the convection boundary at boundaries $j = 0$ and symmetry at $j = J + 1$ are defined in equation (9):

$$w_0^n\left(1 + \frac{\overline{D}_{1/2}^{n-1}}{S . \Delta x}\right) - \frac{\overline{D}_{1/2}^{n-1}}{S . \Delta x} w_1^n = w_e^n \; ; \; w_{J+1}^n - w_J^n = 0 \quad (9)$$

Equation (7) can therefore be written in matrix form (Equation 10):

$$\underline{\underline{A}}^{n-1} \underline{w}^n = \underline{b}^n \quad (10)$$

where the only unknown is the vector $\underline{w}^n$ that contains MC of all points of the sample at time n. Detailed matrix $\underline{\underline{A}}^{n-1}$ and vector $\underline{b}^n$ are given in appendix A.

Optimisation process

Diffusion properties of the presented wood are fitted so that equation (10) accurately represents the experimental results. T and RH measured in the box are directly used as input parameters to calculate w_e using equation (6). Olek and Weres (2001) point out that a so-called inverse method appears to be a valuable tool for determining the coefficients (Eriksson et al. 2006). It appears that the surface exchange coefficients S_{RT} and S_L have a very small impact on the outcome of the equation results. This means that considering the wood's external surface as immediately at equilibrium with the surrounding air is a reasonable assumption regarding the size of the samples. Therefore, S_{RT} and S_L are fixed at 10^5 m.s^{-1}, ensuring no contact resistance. The final unknowns are: (i) diffusion properties D_{0RT}, D_{0L}, k_{DRT}, k_{DL}; (ii) adsorption isotherm parameters w_s, φ_{ad}, a_{ad}. The objective function that has to be minimised is a weighted root mean square (*WRMS*) of the difference between experimental results and the finite difference approximation. As the duration between 2 humidity levels is high and diffusion is not a linear process, there are many more mass measurements when the wood is close to equilibrium compared to right after a new humidity level (i.e., transitory phase). An equilibrium state only depends on w_s, φ_{ad} and a_{ad}, thus only mass measurements in the transitory phase allow to estimate diffusion properties. Consequently, weights are added to the root mean square calculation so that the closer an experimental measurement is to the last humidity level, the bigger is its

weight. This compensates for the fact that these points are fewer in number than those close to the equilibrium state. Mathematically it leads to:

$$WRMS = \sum_{\beta=1}^{B} \sum_{\alpha=1}^{A_\beta} \left(w_{\alpha,\beta}^{meas} - w_{\alpha,\beta}^{est}\right)^2 \times \left[u_{\alpha+1}^{\beta} - u_{\alpha-1}^{\beta}\right] \quad (11)$$

where β is the humidity level number (1 for 43%, 2 for 57%, etc.) ranging from 1 to B and α is the measurement number that is restarted at a new humidity level, ranging from 1 to A_β where A_β depends on the humidity level considered. This leads to the time list: $t_{1,1}, t_{2,1}, \ldots, t_{A_1,1}, t_{1,2}, t_{2,2}, \ldots t_{A_2,2}, \ldots t_{A_B,B}$. $\left(w_{\alpha,\beta}^{meas} - w_{\alpha,\beta}^{est}\right)^2$ is the squared difference between the measured and estimated moisture content, and $\left[u_{\alpha+1}^{\beta} - u_{\alpha-1}^{\beta}\right]$ is the weight factor with:

$$u_{\alpha}^{\beta} = \log\left(t_{\alpha,\beta} - t_{0,\beta}\right) \quad (12)$$

where $t_{0,\beta}$ is the starting time of the humidity level β and $t_{A_\alpha+1,\beta} = t_{0,\beta+1}$ is the starting point of the following humidity level β + 1. This function uses the decrease in the growth rate of the logarithm, which assigns a greater weight to measurement points closer to the beginning of a humidity level. The chosen weight factor ensures a balanced contribution of the different times, expressed in a logarithmic scale, to the fitting process.

The WRMS is calculated for each set of parameters so that the set that minimises the WRMS is considered representative of the material properties. A typical diffusion coefficient ranging is between 10^{-12} and 10^{-8} m².s⁻¹. It is chosen to optimise log(D) instead of its direct value. Indeed, input variations at 10^{-10} are computationally more manageable when expressed logarithmically.

The optimisation is constrained by boundaries for each parameter and uses a Nelder-Mead simplex algorithm. This algorithm is extensively documented in the literature and has already been implemented in Python's Scipy module (Gao and Han 2012). Its selection is based on its ease of use and familiarity to practitioners. However, simplex methods may be influenced by local minima. Therefore, for each species, 10 optimisation processes using 10 random initial values among the boundaries are realised. The selected minimum is the one that is physically the most realistic, in the sense that the anisotropy ratio D_L/D_{RT} should decrease with increasing density. Other optimisation methods, such as differential evolution algorithms, offer a broader scope in terms of exploring the search space and may better ensure convergence to a global optimum (Storn and Price 1997). Gradient-based algorithms are avoided as the WRMS function may not be differentiable. Initial bounds are detailed in appendix B for each parameter of each species.

Table III.
Optimised parameters and weighted root mean square (WRMS) difference of measured and modelled difference for all species

	Silver fir	Douglas fir	Okoume	Padauk	Iroko
D_{RT0} x 10^{-11} [m².s⁻¹]	1.63	2.1	1.34	0.47	1.79
k_{DRT} [-]	8.51	5.77	5.23	1.22	5.29
D_{L0} x 10^{-10} [m².s⁻¹]	9	8.09	10.9	0.6	4.78
k_{DL} [-]	-9.54	-13.1	-13.5	-1.75	-8.76
w_s [%]	24.6	24.4	24.9	15.4	19.4
φ_{ad} [-]	0.67	0.69	0.74	0.67	0.71
a_{ad} [-]	1.63	1.69	1.55	1.65	1.47
$WRMS$ [%]	0.51	0.47	0.35	0.26	0.4

Results and discussion

Fitting of diffusion data

Figure 3 shows the time-evolution of MC, both for experimental and numerical results approximated after optimisation, for all specimens tested in L and RT directions. The optimised diffusion parameters, presented in Table III, accurately describe the evolution of MC with time (WRMS < 0.6% for 225 days).

It is worth noting that w_s is obtained using only adsorption results that did not reach complete saturation, hence cannot be compared with FSP values from the literature. The results highlight the anisotropy with $D_L > D_{RT}$ at any w. This hierarchy has been widely observed by several authors (Agoua and Perré 2010; Mouchot 2002) and is clearly explained by the anatomical configuration that triggers the diffusion process along the tracheids for softwoods and in the vessels for hardwoods. The anisotropy ratio D_L/D_{RT} is between 2 and 70, depending on the considered RH, which is consistent with Siau (1984) that identifies an anisotropy ratio of around 70 at w = 0% and 4 at w = 25% (figure 4). For very dense species, i.e., Padauk and Iroko, the diffusion coefficient is less influenced by moisture content variations.

Figures 5 show the relation between the measured density and diffusion coefficient when w = 8%. Though much more data would be needed to observe a strong correlation, density seems to decrease the diffusion coefficient. This hierarchy corroborates the results of Kouchade (2004) on the effect of density on diffusion, or those of Perré and Turner (2001) who noted that earlywood diffused faster than latewood. Indeed, thicker cell walls and smaller lumen diameters slow down the movement of water vapour. The markedly slower diffusion of Padauk is hence explained by its higher density.

Equilibrium moisture content and hygroscopic table of tropical woods

Based on the optimised parameters, adsorption isotherms are plotted in figure 6. The hygroscopic equilibrium chart of AFNOR (2010) and predicted EMC from Simpson (1973) are added for comparison; they are based on temperate softwood desorption. Iroko and Padauk show systematically lower EMC, possibly explained by the presence of extractives. According to the CIRAD (2015) Tropix database,

Bois et Forêts des Tropiques – ISSN: L-0006-579X
Volume 360 – 2nd quarter – June 2024 – p. 1-12

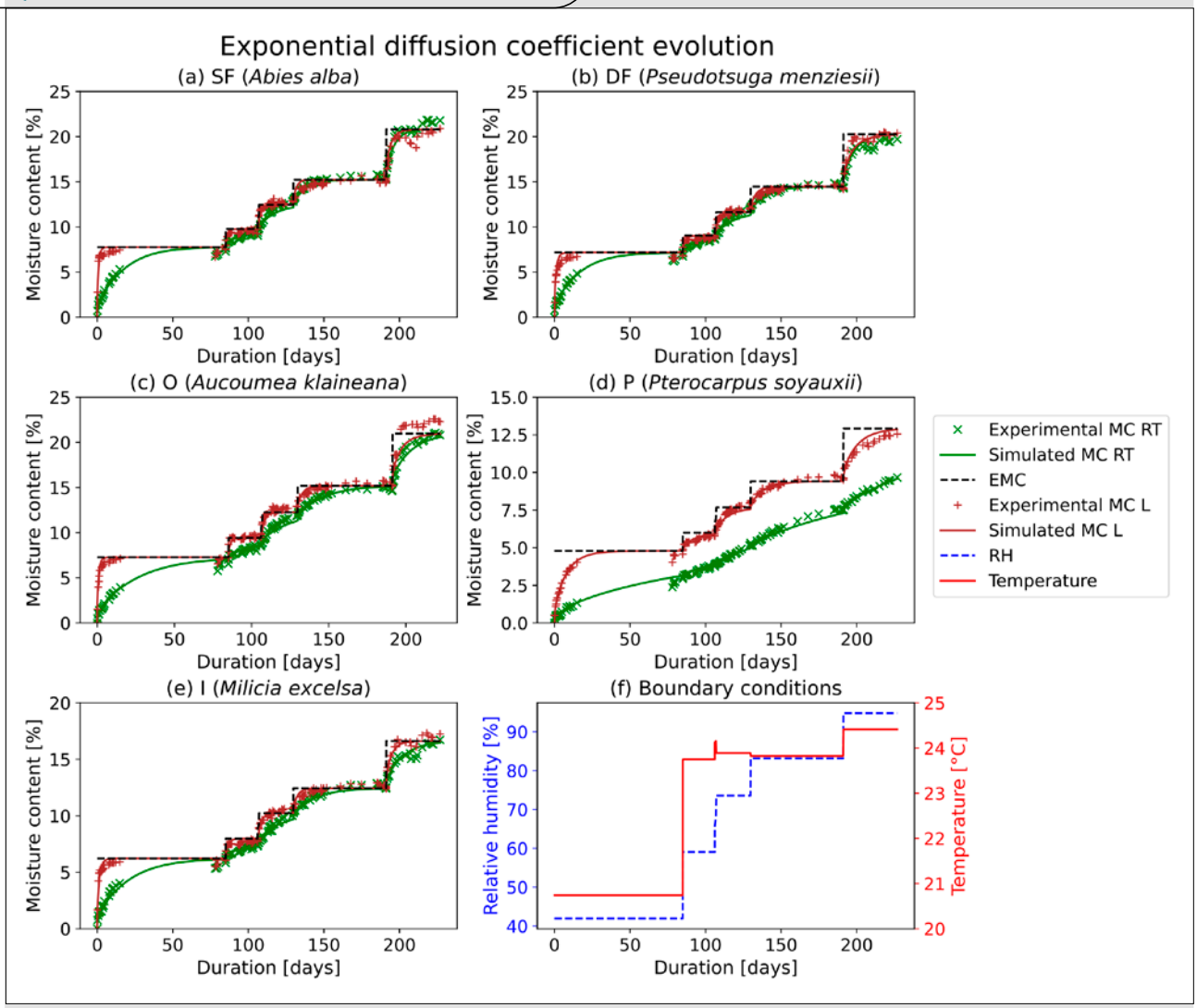

Figures 3.
Diffusion kinetics of tested species in the longitudinal (L, brown) and transverse (RT, green) direction: (a) Silver fir; (b) Douglas fir; (c) Okoume; (d) Padauk; (e) Iroko; (f) Boundary conditions (RH, T). Black dotted line: calculated EMC using equation (6) with optimised adsorption parameters (w_s, a_{ad}, φ_{ad}) and imposed (RH, T); continuous lines: Finite difference approximation; cross: measured MC.

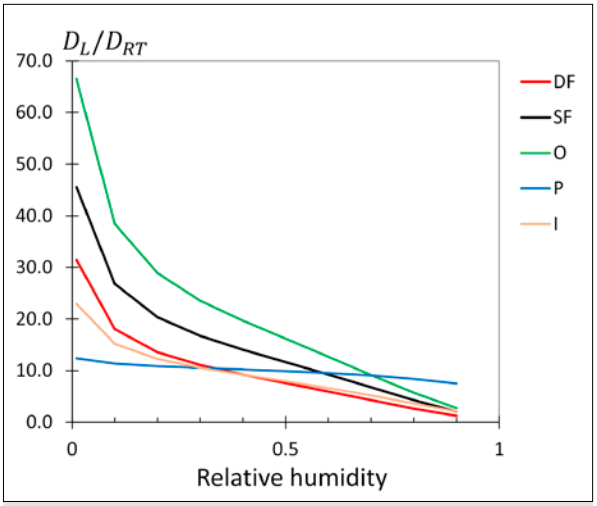

Figure 4.
Anisotropy ratio D_L/D_{RT} as a function of the relative humidity for all species. SF: Silver fir; DF: Douglas fir; O: Okoume; P: Padauk; I: Iroko.

regarding the resistance to fungi and insects such as termites, Padauk is classified as very durable and Iroko as durable to very durable. Okoume and Silver fir have low durability, Douglas fir has low to medium durability. Padauk was shown to contain more extractives than Okoume and Iroko: 9.6 ± 0.9% for Padauk (Mounguengui et al. 2016), 2.1 ± 0.1% for Okoume (Safou-Tchiama 2005), and 5.51 ± 0.11% for Iroko (Gaff et al. 2023). Several studies have shown that the durability of a species is positively related to the extractive content and the type of lignin (Highley 1982; Yamamoto and Hong 1994; Antwi-Boasiako et al. 2010), and Choong and Achmadi (1991) showed that the EMC of extractive-rich wood is lower than that of extractive-poor wood. These results show that model predictions of Simpson (1973) or charts given by NF EN 1995-1-1/NA (2010), valid for temperate softwood desorption, cannot be applied blindly to tropical species. They are particularly not suitable for species that contain many extractives such as Iroko and Padauk.

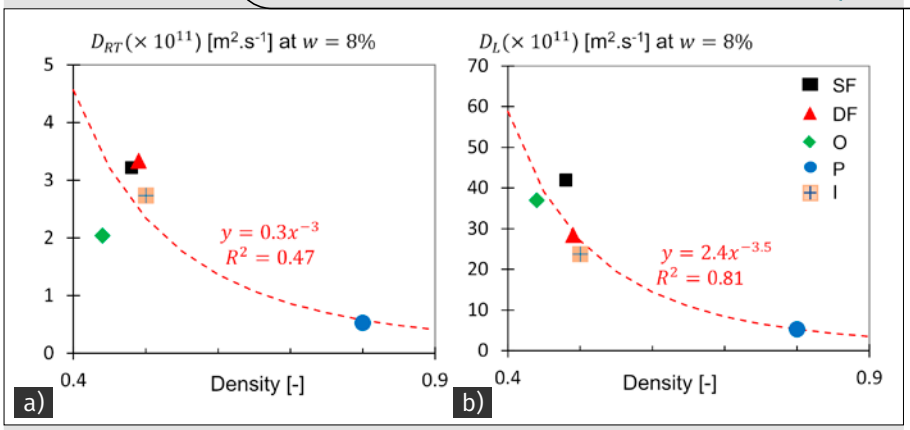

Figures 5.
Diffusion coefficient at w = 8% as a function of the measured density, for both (a) transverse and (b) longitudinal directions.

Conclusion

This paper presents an innovative experimental approach to the study of unidimensional water diffusion in wood and new diffusion data for tropical species. The tests were performed at a temperature of 20-25 °C and successive RH levels: 0, 43, 58, 74, 84, 95%. The frugal adsorption tests coupled with an inverse method based on finite difference approximation of diffusion kinetics allowed the estimation of the diffusion coefficient D_x (m².s⁻¹) and sorption isotherm parameters (w_s, φ_{ad}, a_{ad}) for Padauk, Okoume, Iroko, Silver Fir, and Douglas Fir wood. An optimisation process using Nelder-Mead simplex algorithm is applied. The objective function is a weighted RMS that compensates for the smaller amount of short-term data compared to long-term data. Simplex algorithm may be biased by local minimum, but 10 optimisations are realised, and the most physically significant is chosen and is at least a good approximation. For the European softwoods, the values of the calculated diffusion parameters are close to those of the literature. Among the tropical species tested, only Okoume and Iroko exhibited mass transfer laws similar to temperate woods, while the diffusion of Padauk is slower than Okoume and Iroko. This can be ascribed to the higher density of Padauk wood that requires the water to move through a higher quantity of cell wall and to the high content in extractives that possibly contribute to saturate cell-wall cavities. Furthermore, the anisotropy ratio D_L/D_{RT} of Padauk is less sensitive to MC than one of the other 4 species. The EMC values of Okoume were found to be close to those of European softwoods. However, these EMC values are slightly different from those predicted by the NF EN 1995-1-1/NA (2010) standard and the Simpson's model. This difference can be only partly explained by the fact that sorption hysteresis is not considered in these models. The sorption isotherm parameters of Padauk and Iroko are significantly different than those of European softwood and that is justified by the extractive content of these tropical species. Because of the very different hydric behaviour highlighted for tropical species in the future, it will be necessary to develop specific models for these species as well as specific hygroscopic equilibrium charts.

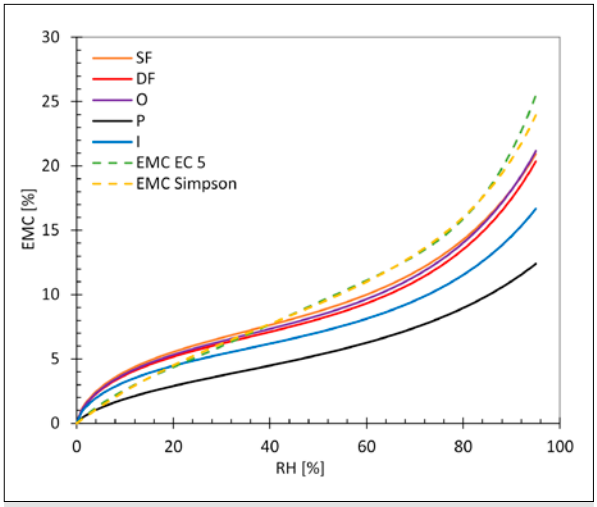

Figure 6.
Equilibrium moisture content of each species, green dashed-line NF EN 1995-1-1/NA (2010) model (EMC EC 5); yellow dashed-line Simpson (1973) model (EMC Simpson). SF: Silver fir; DF: Douglas fir; O: Okoume; P: Padauk; I: Iroko; EMC: Equilibrium moisture content [%]; RH: Air relative humidity [%].

Acknowledgements
The authors would like to take this opportunity to thank the Biology Department of Polytech Clermont Ferrand for the provision of saline solutions for this work.

Funding
The funding of both the Gabonese and Auvergne-Rhône-Alpes region scholarships makes the Ph.D. possible and enables us to pay for experimental equipment. Besides, the Hub-Innovergne program of the Clermont Auvergne University helped pay for the experimental device.

Access to research data
All Excel sheets of the measurements and python scripts of the analysis concerning the work presented in this article are publicly available on Zenodo: https://zenodo.org/records/13839289
Please, think to inform authors and to cite the dataset as: BONTEMPS A., 2024. Data for article BFT-Assekoetal2024_diffusion_of_tropical_hardwoods [Data set]. Zenodo. https://doi.org/10.5281/zenodo.13839289

Bois et Forêts des Tropiques – ISSN: L-0006-579X
Volume 360 – 2nd quarter – June 2024 – p. 1-12
RESEARCH / DIFFUSION PROPERTIES OF GABONESE TROPICAL HARDWOODS

Appendix A.
Finite-difference calculation.

Second Fick's law for unidimensional problem is approximated using implicit Euler scheme that gives the matrix problem from equation (10):

$$\underline{\underline{A}}^{n-1}\underline{w}^{n} = \underline{b}^{n} \qquad (A1)$$

where $\underline{\underline{A}}^{n-1}$ is:

$$\begin{bmatrix} 1+F_2\overline{D}_{1/2}^{n-1} & -F_2\overline{D}_{1/2}^{n-1} & 0 & 0 & & \\ -\theta F_1\overline{D}_{1/2}^{n-1} & 1+\theta F_1(\overline{D}_{1/2}^{n-1}+\overline{D}_{3/2}^{n-1}) & -\theta F_1\overline{D}_{3/2}^{n-1} & 0 & \cdots & 0 \\ 0 & -\theta F_1\overline{D}_{3/2}^{n-1} & 1+\theta F_1(\overline{D}_{3/2}^{n-1}+\overline{D}_{5/2}^{n-1}) & -\theta F_1\overline{D}_{5/2}^{n-1} & & \\ & \vdots & & \ddots & \vdots & \\ & 0 & & \cdots & -\theta F_1\overline{D}_{I-1/2}^{n-1} & 1+\theta F_1(\overline{D}_{J-1/2}^{n-1}+\overline{D}_{J+1/2}^{n-1}) & -\theta F_1\overline{D}_{I+1/2}^{n-1} \\ & & & & 0 & -1 & 1 \end{bmatrix}$$

with $F_1 = \Delta t/\Delta x^2$, $F_2 = 1/(S_x\Delta x)$ and:

$$(\underline{b}^{n})^{T} = \left[w_e^n \quad 0 \quad \cdots \quad F_1(1-\theta)\left[\overline{D}_{j+\frac{1}{2}}^{n-1}(w_{j+1}^{n-1}-w_j^{n-1}) - \overline{D}_{j-\frac{1}{2}}^{n-1}(w_j^{n-1}-w_{j-1}^{n-1})\right] + w_j^{n-1} \quad \cdots \quad 0\right] ;$$

$$(\underline{w}^{n})^{T} = [w_0 \quad w_1 \quad \cdots \quad w_J \quad w_{J+1}]^n \qquad (A3)$$

All above parameters are defined in Physics of diffusion kinetics and finite difference approximation sections.

Appendix B.
Boundaries for the constrained optimisation process.

Boundaries are centered on physically coherent values based on literature (Alkadri 2020; Asseko Ella 2022; Bontemps 2023 ; Cirad (2015) Tropix Database for w_s), table B1:

Table B1.
Centered values for the boundaries of the constrained optimisation process.

	Silver fir	Douglas fir	Okoume	Padauk	Iroko
log (D_{RT0})	-10.284	-10.441	-10.355	-11.26	-10.42
log (D_{L0})	-9.547	-9.752	-9.697	-10.31	-9.658
w_s	0.256	0.248	0.257	0.141	0.197
φ_{ad}	0.82	0.82	0.73	0.78	0.76
a_{ad}	1.435	1.435	1.636	1.16	1.413

Then boundaries are fixed such that, considering the logarithm of the optimised value, the minimum (2/3) of the centered value and the maximum is (4/3) of the centered value. This gives tremendous range thanks to the logarithm function. The boundaries of k_{DL} and k_{DRT} are: [1.10^{-4}, 30] based on the values proposed by Siau (1984).

Appendix C.
Variations in relative humidity in the box during an experimental phase and when the trap is opened.

This figure shows the hydric condition of the box during the measurements and when the trap is opened to change the RH. The figures C1a and C1c show that the variations in RH during the measurements (opening of the Silicon caps) are low and have a small influence on the measurements. In those figures we can see that the average RH values are 42.16% ± 0.40 RH (figure C1a) and 57.24% ± 0.80 RH (figure C1b) and are very close to the values predicted by the standard. When the trap is opened, the time taken for RH to stabilise is around 3 to 4 hours (figure C1c).

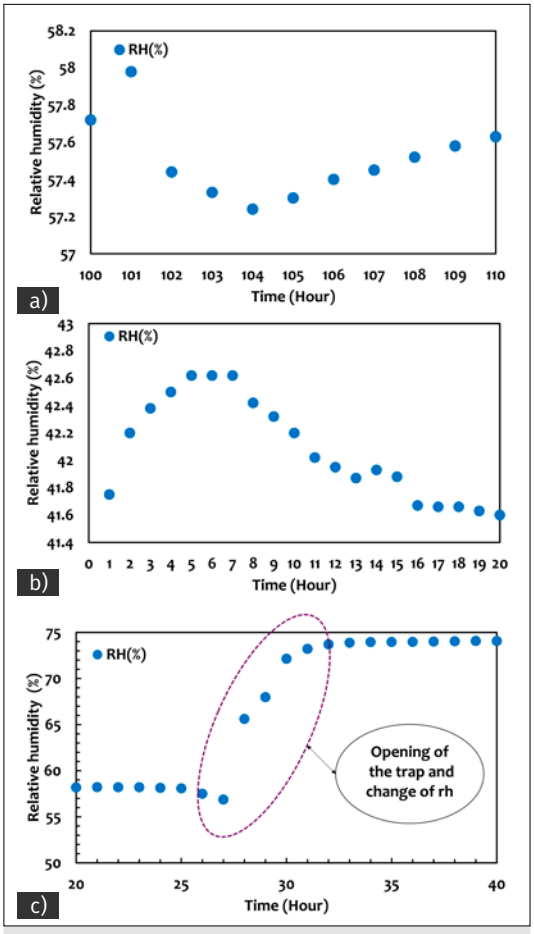

Figures C1.
Hydric conditions of the box during the measurements: (a) 42% RH; (b) 58% RH; (c) opening of the trap for the change of RH.

References

Agoua E., Perré P., 2010. Mass transfer in wood: Identification of structural parameters from diffusivity and permeability measurements. Journal of Porous Media, 13 (11): 1017-1024. https://doi.org/10.1615/JPorMedia.v13.i11.80

Agoua E., Zohoun S., Perré P., 2001. A double climatic chamber used to measure the diffusion coefficient of water in wood in unsteady-state conditions: Determination of the best fitting method by numerical simulation. International Journal of Heat and Mass Transfer, 44 (19): 3731-3744. https://doi.org/10.1016/S0017-9310(01)00022-9

Alkadri A., Jullien D., Arnould O., Rosenkrantz E., 2020. Hygromechanical properties of grenadilla wood (*Dalbergia melanoxylon*). Wood Science and Technology 54: 1269-1297. https://doi.org/10.1007/s00226-020-01215-z

Antwi-Boasiako C., Barnett J. R., Pitman A. J., 2010. Relationship between total extractive content and durability of three tropical hardwoods exposed to *Coriolus versicolor* (Linnaeus) Quelet. Journal of the Indian Academy of Wood Science, 7 (1–2): 9-13. https://doi.org/10.1007/s13196-010-0002-3

Asseko Ella M., 2022. Effet de la mécanosorption et de l'hygroviscoélasticité sur la fissuration des feuillus gabonais et résineux européens. PhD Thesis, Université Clermont Auvergne, HAL, 206 p. https://theses.hal.science/tel-03953610

Benoit Y., Legrand B., Tastet V., 2019. Calcul des structures en bois – Guide d'application des Eurocodes 5 (structures en bois) et 8 (séismes) - Assemblage de pieds de poteaux. 4ème édition, Éditions Eyrolles, 540 p.

Bontemps A., 2023. Comportement mécanique des éléments de structure en bois de sapin pectiné soumis à un environnement variable. PhD Thesis, Université Clermont Auvergne, 264 p. https://theses.hal.science/tel-04151652

Choong E., Achmadi S., 1991. Effects of extractives on moisture sorption and shrinkage in tropical woods. Wood and fiber science, 23 (2): 185-196. https://wfs.swst.org/index.php/wfs/article/view/399

Choong E. T., Skaar C., 1972. Diffusivity and surface emissivity in wood drying. Wood and Fiber Science, 4 (2): 80-86. https://wfs.swst.org/index.php/wfs/article/view/399

CIRAD, 2015. Tropix 7 (version 7.5.1) – The main thecnological characteristics of 245 tropical wood species. Software database, CIRAD. https://doi.org/10.18167/74726F706978

Comstock G. L., 1963. Moisture diffusion coefficients in wood as calculated from adsorption, desorption, and steady state data. Forest Product Journal, 13 (3): 97-103. https://www.cabidigitallibrary.org/doi/full/10.5555/19636605512

Engonga Edzang A. C., Pambou Nziengui C. F., Ekomy Ango S., Ikogou S., Moutou Pitti R., 2020. Comparative studies of three tropical wood species under compressive cyclic loading and moisture content changes. Wood Material Science and Engineering, 16 (3): 193-203. https://doi.org/10.1080/17480272.2020.1712739

Eriksson J., Johansson H., Danvind J., 2006. Numerical determination of diffusion coefficients in wood using data from CT-scanning. Wood and fiber science, 2: 334-344. https://wfs.swst.org/index.php/wfs/article/view/1405

Gaff M., Kubovský I., Sikora A., Kačíková D., Li H., Kubovský M., et al., 2023. Impact of thermal modification on color and chemical changes of African padauk, merbau, mahogany, and iroko wood species reviews on advanced materials science, 62 (1): 20220277. https://doi.org/10.1515/rams-2022-0277

Gao F., Han L., 2012. Implementing the Nelder-Mead simplex algorithm with adaptive parameters. Computational Optimization and Applications, 51 (1): 259-277. https://doi.org/10.1007/s10589-010-9329-3

Highley T. L., 1982. Influence of type and amount of lignin on decay by *Coriolus versicolor*. Canadian Journal of Forest Research, 12 (2): 435-438. https://doi.org/10.1139/x82-065

Kollman F. F. P., Cöte W. A., 1968. Principles of wood science and technology. 1. solid wood. Springer-Verlag, 592 p. https://link.springer.com/book/10.1007/978-3-642-87928-9

Kouchade A. C., 2004. Mass diffusity of wood determined by inverse method from electrical resistance measurement in unsteady state. PhD thesis, ENGREF (AgroParisTech), 139 p. https://pastel.hal.science/pastel-00000888/file/clement_these.pdf

Liu M., Peng L., Lyu S., Lyu J., 2020. Properties of common tropical hardwoods for fretboard of string instruments. Journal of Wood Science, 66 (1): 14. https://doi.org/10.1186/s10086-020-01862-7

Manfoumbi Boussougou N., Nguyen T. A., Angellier N., Dubois F., Ulmet L., Sauvat N., 2014. Experimental and numerical aspects in diffusion process characterization in tropical species. European Journal of Environmental and Civil Engineering, 18 (9): 963-982. https://doi.org/10.1080/19648189.2014.917993

Merakeb S., Dubois F., Petit C., 2009. Modeling of sorption hysteresis in hygroscopic materials'. Comptes Rendus – Mécanique, 337 (1): 34-39. https://doi.org/10.1016/j.crme.2009.01.001

Mounguengui S., Saha Tchinda J. B., Ndikontar M. K., Dumarçay S., Attéké C., Perrin D., et al., 2016. Total phenolic and lignin contents, phytochemical screening, antioxidant and fungal inhibition properties of the heartwood extractives of ten Congo Basin tree species. Annals of Forest Science, 73 (2): 287-296. https://doi.org/10.1007/s13595-015-0514-5

Mouchot N., 2002. Étude expérimentale et modélisation des transports diffusionnels de l'eau dans le domaine hygroscopique des bois de hêtre et d'épicéa. Thèse de doctorat, Université Henri Poincaré - Nancy 1, 232 p. https://theses.fr/2002NAN10284

NF EN ISO 483, 2006. Plastics-small enclosures for conditioning and testing using aqueous solutions to maintain the humidity at a constant value. AFNOR publishing, 10 p.

NF EN 1995-1-1/NA, 2010. Eurocode 5: Design and calculation of wooden structures - Part 1-1: general - Common rules and rules for buildings - National annex to NF EN 1995-1-1:2008 - General - Common rules and rules for buildings. AFNOR publishing, 10 p.

Olek W., Weres J., 2001. The inverse method for diffusion coefficient identification during water sorption in wood. Holzforschung, 59 (1): 38-45. https://doi.org/10.1515/HF.2005.007

Perré P., Turner I., 2001. Determination of the material property variations across the growth ring of softwood for use in a heterogeneous drying model. Part 2. Use of homogenisation to predict bound liquid diffusivity and thermal conductivity. Holzforschung, 55 (4): 417-425. https://doi.org/10.1515/HF.2001.069

Rosen H. N., 1978. The Influence of External Resistance on Moisture Adsorption Rates in Wood. Wood and Fiber Science, 10 (3): 218-228. https://wfs.swst.org/index.php/wfs/article/view/1228

Safou-Tchiama R., 2005. Caractérisation physico-chimique stabilité supramoléculaire et réactivité chimique de quelques essences tropicales. PhD thesis, Université Bordeaux 1, 175 p. https://theses.fr/2005BOR13095

Siau J. F., 1984. Steady-State Moisture Movement. In: Transport Processes in Wood. Springer Series in Wood Science, vol 2. Springer, 151-174. https://doi.org/10.1007/978-3-642-69213-0_6

Siau J. F., Avramidis S., 1996. The surface emission coefficient of wood. Wood and Fiber Science, 28 (2): 178-185. https://wfs.swst.org/index.php/wfs/article/view/1538

Simo-Tagne M., Rémond R., Rogaume Y., Zoulalian A., Bonoma B., 2016. Sorption behavior of four tropical woods using a dynamic vapor sorption standard analysis system. Maderas, Ciencia y Tecnologia, 18 (3): 403-412. https://doi.org/10.4067/S0718-221X2016005000036

Simpson W., 1973. Predicting equilibrium moisture content of wood by mathematical models. Wood and Fiber, 5 (1): 41-49. https://wfs.swst.org/index.php/wfs/article/view/740

Stamm A. J., 1959. Bound-water diffusion into wood in the fiber direction. Forest Products Journal, 9: 27-32. https://eurekamag.com/research/013/972/013972514.php

Storn R., Price K., 1997. Differential evolution – A simple and efficient heuristic for global optimization over continuous spaces. Journal of global optimization, 11: 341-359. https://doi.org/10.1023/A:1008202821328

Thybring E. E., Fredriksson M., Zelinka S. L., Glass S. V., 2022. Water in Wood: A Review of Current Understanding and Knowledge Gaps. Forests, 13 (12): 2051. https://doi.org/10.3390/f13122051

Varnier M., 2019. Comportement thermo-hygro-mécanique différé des feuillus : des sciences du bois à l'ingénierie. Thèse de doctorat, University of Limoges, HAL, Id: tel-02303304. https://theses.hal.science/tel-02303304v1/file/2019LIMO0035.pdf

Varnier M., Sauvat N., Ulmet L., Montero C., Dubois F., Gril J., 2020. Influence of temperature in a mass transfer simulation: application to wood. Wood Science and Technology, 54 (4): 943-962. https://doi.org/10.1007/s00226-020-01197-y

Yamamoto K., Hong L. T., 1994. A laboratory method for predicting the durability of tropical hardwoods. Japan Agricultural Research Quarterly (JARQ), 28 (4): 268-275. https://www.jircas.go.jp/sites/default/files/publication/jarq/28-4-268-275_0.pdf

Asseko Ella et al. – Credit authorship contribution statement

Contributor role	Contributor names
Conceptualisation	J. Gril, R. Moutou Pitti, G. Godi, É. Fournely
Data Curation	M. Asseko Ella
Formal Analysis	A. Bontemps, M. Asseko Ella, J. Gril
Funding Acquisition	R. Moutou Pitti
Investigation	M. Asseko Ella, J. Gril
Methodology	G. Godi, J. Gril, M. Asseko Ella, A. Bontemps
Project Administration	R. Moutou Pitti, J. Gril
Resources	G. Godi, R. Moutou Pitti
Software	A. Bontemps, G. Godi, J. Gril
Supervision	J. Gril, R. Moutou Pitti, G. Goli, S. Ikogou, É. Fournely
Validation	J. Gril, R. Moutou Pitti, G. Goli
Visualisation	A. Bontemps, M. Asseko Ella
Writing – Original Draft Preparation	M. Asseko Ella, A. Bontemps
Writing – Review & Editing	J. Gril, G. Godi, R. Moutou Pitti

Bois et Forêts des Tropiques - Revue scientifique du Cirad -

Cirad - Campus international de Baillarguet,
34398 Montpellier Cedex 5, France
Contact : bft@cirad.fr - ISSN : L-0006-579X